Mechanism of the $^{12}C(^{24}Mg,^{12}C^{12}C)^{12}C$ breakup reaction: Direct vs compound

S. M. Singer, W. N. Catford, G. J. Gyapong, and M. Shawcross
School of Physics and Chemistry, University of Surrey, Guildford, Surrey GU2 7XH, United Kingdom

N. M. Clarke, N. Curtis, M. Freer, B. R. Fulton, S. J. Hall, R. A. Le Marechal, M. J. Leddy, J. S. Pople, G. Tungate, and R. P. Ward*
School of Physics and Astronomy, University of Birmingham, Edgbaston, Birmingham B15 2TT, United Kingdom

W. D. M. Rae and P. M. Simmons
Department of Physics, University of Oxford, Nuclear Physics Laboratory, Keble Road, Oxford OX1 3RH, United Kingdom

S. P. G. Chappell, S. P. Fox, C. D. Jones, P. Lee, and D. L. Watson
Department of Physics, University of York, York YO1 5DD, United Kingdom
(Received 1 October 1999; revised manuscript received 18 July 2000; published 10 October 2000)

A backward angle measurement has been made of the angular distribution for the states in ^{24}Mg that decay by symmetric fission to $^{12}C + {}^{12}C$ in the $^{12}C(^{24}Mg,^{12}C^{12}C)^{12}C$ reaction. A comparison with previous very forward angle measurements indicates a substantial asymmetry in the angular distribution, averaged over a range of excitation energies in ^{24}Mg. The observed degree of forward-backward asymmetry is reasonably well reproduced by coupled channels calculations assuming a direct inelastic scattering mechanism. Combining this information with previous measurements of the energy systematics supports direct inelastic excitation as the most likely reaction mechanism leading to the fissioning levels.

PACS number(s): 24.10.−i, 25.70.−z, 27.30.+t

I. INTRODUCTION

The scattering of ^{24}Mg from ^{12}C has been observed to excite states in ^{24}Mg that decay by symmetric fission into $^{12}C+{}^{12}C$ [1] and states that decay by near symmetric fission into $^{16}O+{}^{8}Be$ [2]. These special states that decay into large clusters are of particular spectroscopic interest and a number of studies have been reported on their structure [3,4] and on their relation to the resonances in $^{12}C+{}^{12}C$ scattering [5]. However, of equal importance is an understanding of the reaction mechanism by which such unusual structures can be produced. Indeed an understanding of the reaction mechanism can in turn aid the understanding of the spectroscopy of the states.

In a previous work, Gyapong *et al.* [6] attempted to determine the reaction mechanism by measuring the yield of the breakup states as a function of the beam energy. The experimental results were compared with the predictions of four reaction mechanisms: a compound statistical process; a compound resonant process; a coupled-channels inelastic excitation; and direct ^{12}C transfer. The statistical model calculation was performed with the computer code STATIS [7], which uses the Hauser-Feshbach formalism and assumes the reaction to proceed via a fully equilibrated compound nucleus. This calculation did not match the experimental results and a statistical fusion-evaporation process was ruled out by the authors. The resonant model calculation followed a suggestion by Rae and Merchant [8] based on their cranked α cluster model calculations for *sd*-shell nuclei. In this model, the reaction proceeds via resonant states in ^{36}Ar which are part of a 3:1 deformed band which has a structural overlap with a deformed band in ^{24}Mg. The states are 50–70 MeV above the particle decay threshold and thus their widths are expected to be several MeV. The results of this calculation did agree with the measurements. The inelastic coupled-channels calculations were performed with the computer code FRESCO [9] assuming a direct excitation of ^{24}Mg from the ground-state rotational band into a band based on a 3:1 state and consistent with the band observed by Fulton *et al.* [10] in their measurement of the breakup reaction. These results also agreed with the experimental energy dependence. The final calculations, which used the computer code CHUCK [11] and assumed a direct ^{12}C transfer from the ^{24}Mg to the ^{12}C, failed to match the observations.

The conclusion drawn by Gyapong *et al.* was that the observed energy dependence of the ^{24}Mg breakup reaction was consistent with either a resonant or a direct inelastic excitation process. However, the energy variation alone was not sufficient to distinguish between these.

Another key indicator of the reaction mechanism is the angular distribution of the reaction products. There is limited information about the angular distribution for the $^{12}C(^{24}Mg,^{12}C^{12}C)^{12}C$ reaction [12]. These data showed that the yield is very forward peaked with $d\sigma/d\Omega$ falling by a factor of 100 between θ^* of 0° and 20°, where θ^* is the center-of-mass scattering angle of the excited ^{24}Mg nucleus. The laboratory cross section was measured to be (1.07 ± 0.12) mb sr^{-2} averaged over this angular range. However, this limited range of θ^* is insufficient to distinguish reliably between different reaction mechanisms by way of $d\sigma/d\Omega$.

Broadly speaking, compound nuclear or resonance models predict cross sections that are symmetric about $\theta^*=90°$,

*Present address: School of Chemistry and Physics, Keele University, Keele, Staffordshire ST5 5BG, U.K.

TABLE I. Summary of parameters and results for the forward angle experiment [12] together with the parameters for the present experiment.

Reaction	^{12}C(^{24}Mg,^{12}C^{12}C)^{12}C	^{24}Mg(^{12}C,^{12}C^{12}C)^{12}C
Beam energy (MeV)	170	85
Detector position (a)	$11°24'$	22°
Detector position (b)	$-12°27'$	$-22°$
Detector size (mm^2)	10×10	50×50
Detector-target distance (mm)	120	170
Target thickness ($\mu g\,cm^{-2}$)	400	289
Integrated beam current (mC)	3.11	2.59
Counts in Q_{ggg} peak	1644	
Cross section ($mb\,sr^{-2}$)	1.07 ± 0.12	

whereas direct reaction models tend to predict very asymmetric distributions (deviations from this simple average behavior can arise under certain circumstances, as will be discussed in Sec. IV). Thus, although the data taken at forward angles are unable to separate the predictions of different reaction mechanisms, when forward and backward angle measurements are compared, the different predictions should become much easier to distinguish.

In this paper, we report the results of a measurement of the angular distribution close to $\theta^*=180°$ to allow the two extremes of the angular distribution to be compared. In order to achieve this, the reaction kinematics were reversed and forward angles measured in the reaction ^{24}Mg(^{12}C,^{12}C^{12}C)^{12}C. This was necessary as, if a ^{24}Mg beam were to be used, the breakup ^{12}C nuclei corresponding to backward angle scattering would be too low in energy to be detected. Experimental parameters such as beam energy and detector angles were chosen to ensure that the new measurements would be directly comparable with the forward angle experiment [12] that used a ^{24}Mg beam. These parameters are shown in Table I.

II. EXPERIMENTAL DETAILS

The measurements were performed using an 85 MeV ^{12}C beam from the 14UD accelerator at the Australian National University. The ^{12}C ions from the breakup were detected in two gas-hybrid detectors. Each detector consisted of a 5 cm$\times$5 cm position sensitive silicon strip detector placed behind a longitudinal ionization chamber [13]. Each detector was capable of recording the energy and position of a particle, as well as providing particle identification. The detectors were set at 22° on either side of the beam and placed 170 mm from the target, a 289 $\mu g\,cm^{-2}$ ^{24}Mg foil.

The analysis technique is described in Ref. [13]. Briefly, events in which two ^{12}C nuclei were simultaneously detected were selected for analysis. Their momenta were calculated from their measured energies and angles and the momentum of the undetected final state ^{12}C was deduced using conservation of momentum. Adding the energy of the three final state particles together gave the total final-state energy (E_{tot}) from which the Q value could be determined. The E_{tot} spectrum is shown in Fig. 1. The Q value for producing all three ^{12}C nuclei in their ground state (referred to as Q_{ggg}) is -13.93 MeV, and that for producing two ^{12}C nuclei in their ground state, and one in its 4.4 MeV excited state (referred to as Q_{gg}) is -18.33 MeV.

The Q_{gg} peak is clearly visible in Fig. 1 and evidence of a Q_{ggg} peak is also seen. Since the width of the Q_{ggg} peak is not well defined, the Q_{gg} and Q_{ggg} peaks have been fitted simultaneously, keeping the widths of the Gaussian line shapes fixed for both peaks. This gave a Q_{ggg} peak area of (93 ± 22) counts and a width of 1.0 MeV. The fitted line shapes are shown in Fig. 1 together with a second-order fit to the underlying background. It is noted that the Q_{gg} peak will, in general, be Doppler broadened due to γ decay of the excited fragment in flight. However, this effect is estimated to contribute less than 10% (less than $\frac{1}{2}$ channel in Fig. 1) to the width of the Q_{gg} peak and therefore is not expected to affect the above result, to within the accuracy of the fitting procedure.

III. ANALYSIS

Although it is possible to convert the number of counts in the Q_{ggg} peak into a laboratory cross section of (0.64 ± 0.15)

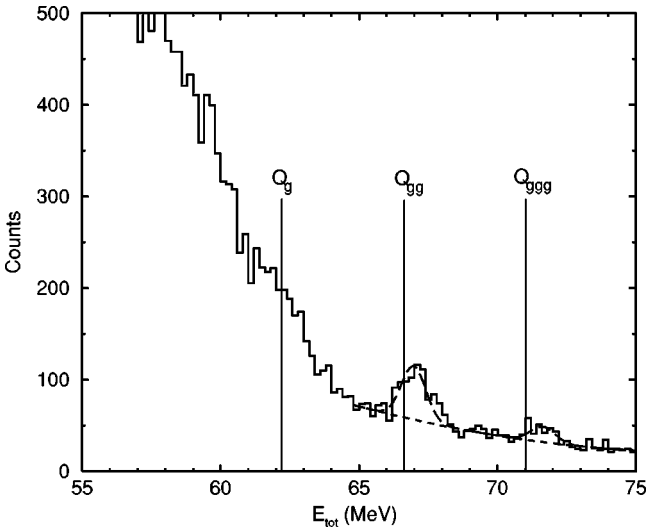

FIG. 1. E_{tot} spectrum generated for the present experiment showing peaks at the energies predicted for Q_{ggg} and Q_{gg} events. Gaussian fits to these peaks are indicated together with a second-order fit to the underlying background.

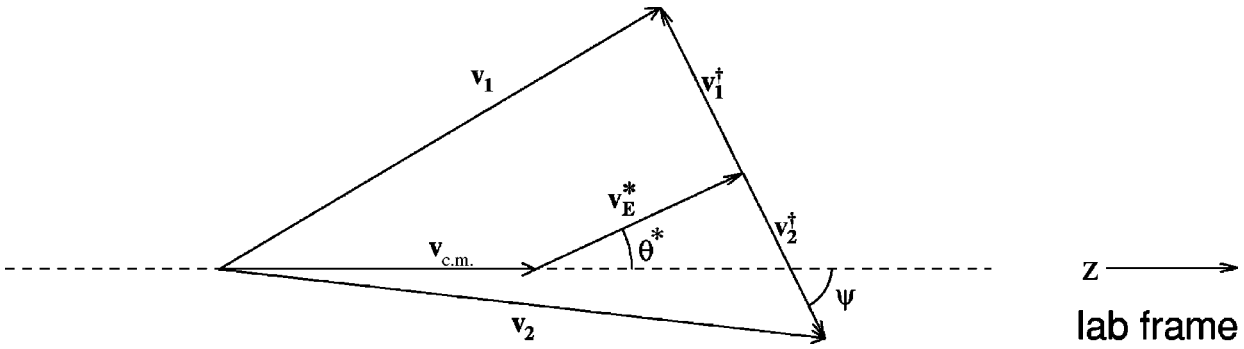

FIG. 2. Definitions of terms used in the phase-space mapping.

μb sr^{-2}, this simple figure is not useful for comparison with the previously quoted forward angle cross section for a number of reasons. First, because the two measurements have been carried out under different kinematic conditions, the solid angle transformations to the center-of-mass system are different. Second, the detectors did not cover identically mirror symmetric regions of angles at forward and backward angles. Finally, only the exclusive yield to the $^{12}C+^{12}C$ channel has been measured and not that from a specific excitation in ^{24}Mg. The excitation energy ranges covered in the two measurements are different, being determined by the angular coverage of the detectors and the detection energy threshold.

The procedure used in this analysis was to apply a software cut to the backward angle data to reduce its excitation energy and angular range down to just that of the forward angle experiment. By this means identical sections of the forward and backward angular distributions could be compared over identical excitation energy ranges in the scattered ^{24}Mg nucleus.

Any event detected in a breakup measurement can be categorized by the velocity vectors of the two detected particles. It is possible to define a phase space of all possible values of these vectors that can be obtained in the reaction. This laboratory phase space will be denoted as Σ_l. It is a five-dimensional phase space, though it is most easily described with the six variables v_1, θ_1, ϕ_1, v_2, θ_2, and ϕ_2 where v is the laboratory velocity of each particle, and θ and ϕ are the emission angles in the lab frame. Conservation of momentum and energy mean that these six variables are correlated in such a way that the phase space is only five dimensional. In addition, any event can be categorized uniquely by a set of five center of mass variables. These variables are θ^*, ϕ^*, ψ, χ, and E_x. θ^* and ϕ^* define the center-of-mass scattering angle of the excited ^{24}Mg nucleus, while ψ and χ define the angle of the breakup ^{12}C nuclei in the ^{24}Mg center-of-mass frame. E_x is the excitation energy of the ^{24}Mg nucleus. θ^* and ψ are shown in Fig. 2. These five variables define a five-dimensional phase space denoted Σ_c. There is a mapping between Σ_l and Σ_c, so that any point in one phase space can be mapped onto a point in the other phase space.

Using the notation in Fig. 2, the mapping between Σ_c and Σ_l is given by

$$\mathbf{v_1}=\mathbf{v_1^\dagger}+\mathbf{v_E^*}+\mathbf{v_{c.m.}}, \tag{1}$$

$$\mathbf{v_2}=\mathbf{v_2^\dagger}+\mathbf{v_E^*}+\mathbf{v_{c.m.}}, \tag{2}$$

where

$$\mathbf{v_1}=v_1\begin{pmatrix}\sin\theta_1\cos\phi_1\\ \sin\theta_1\sin\phi_1\\ \cos\theta_1\end{pmatrix}, \tag{3}$$

$$\mathbf{v_2}=v_2\begin{pmatrix}\sin\theta_2\cos\phi_2\\ \sin\theta_2\sin\phi_2\\ \cos\theta_2\end{pmatrix}, \tag{4}$$

$$\mathbf{v_{c.m.}}=\sqrt{\frac{2m_pE_{c.m.}}{m_t(m_p+m_t)}}\begin{pmatrix}0\\ 0\\ \delta\end{pmatrix}, \tag{5}$$

$$\mathbf{v_E^*}=\sqrt{\frac{2m_u(E_{c.m.}+Q_1-E_x)}{(m_1+m_2)(m_p+m_t)}}\begin{pmatrix}\sin\theta^*\cos\phi^*\\ \sin\theta^*\sin\phi^*\\ \cos\theta^*\end{pmatrix}, \tag{6}$$

$$\mathbf{v_1^\dagger}=\sqrt{\frac{2m_2(E_x+Q_2)}{m_1(m_1+m_2)}}\begin{pmatrix}-\sin\psi\cos\chi\\ -\sin\psi\sin\chi\\ -\cos\psi\end{pmatrix}, \tag{7}$$

$$\mathbf{v_2^\dagger}=\sqrt{\frac{2m_1(E_x+Q_2)}{m_2(m_1+m_2)}}\begin{pmatrix}\sin\psi\cos\chi\\ \sin\psi\sin\chi\\ \cos\psi\end{pmatrix}. \tag{8}$$

Here, m_p is the mass of the projectile, m_t is the mass of the target, m_1 is the mass of particle 1, m_2 is the mass of particle 2, m_u is the mass of the undetected particle $(m_p+m_t-m_1-m_2)$, $E_{c.m.}$ is the center-of-mass energy $[E_{beam}m_t/(m_p+m_t)]$, Q_1 is the Q value of the first stage of the reaction (the scattering), Q_2 is the Q value of the second stage of the reaction (the breakup), and δ is $+1$ for a forward angle experiment and -1 for a backward angle experiment. The notation Σ_f will be used for the laboratory phase space for the earlier, forward angle, experiment, and Σ_b for the present, backward angle, experiment.

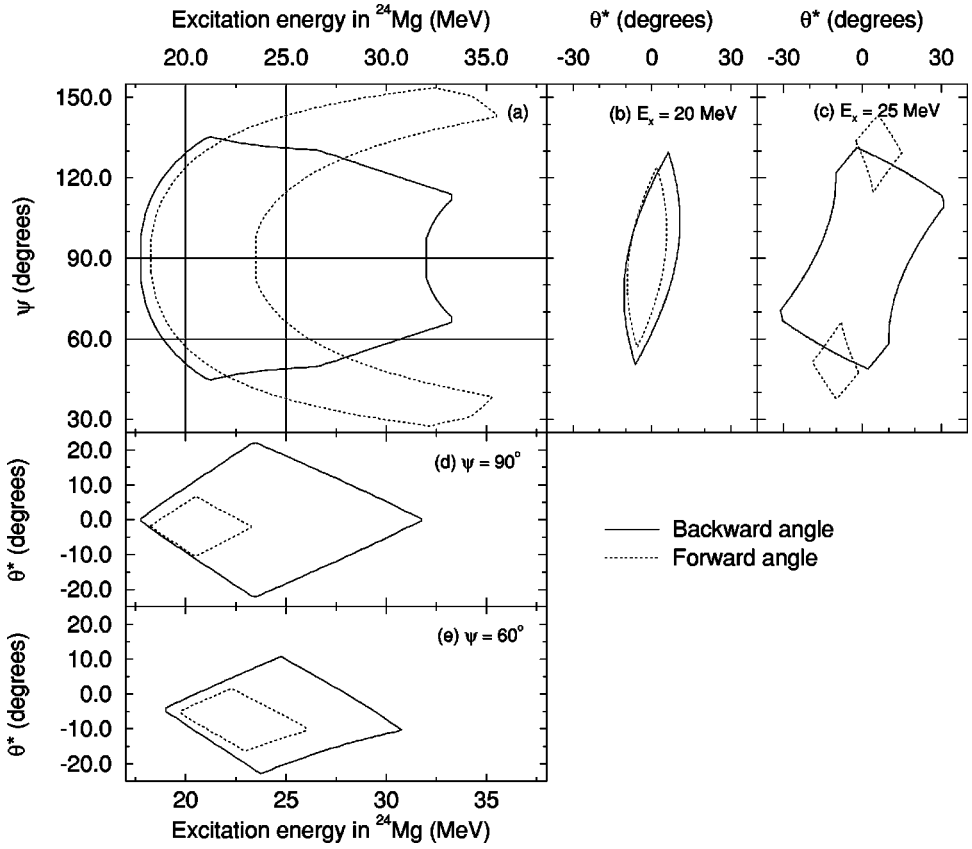

FIG. 3. A selection of views comparing the phase-space coverage of the two experiments. The coverage of the backward angle experiment has been reflected to allow comparison with the forward angle experiment. See the text for details of views (a)–(e).

For each forward angle point in Σ_c, an equivalent backward angle point can be defined. The transformation from one point to the other is

$$(\theta^*,\phi^*,\psi,\chi,E_x) \rightarrow (180^\circ-\theta^*,180^\circ+\phi^*,180^\circ-\psi,180^\circ+\chi,E_x). \tag{9}$$

An angular distribution is mirror symmetric if, and only if, this transformation leaves it unchanged. Ideally, the cross sections of the two experiments would be compared as a function of the coordinates in Σ_c. Unfortunately, due to the low counting rate in the present experiment, this was not feasible. Instead the integrated cross sections over mirror symmetric volumes of Σ_c were calculated. While an asymmetric angular distribution could, in principle, conspire to give identical integrated cross sections, if different values are obtained then this uniquely identifies an asymmetric distribution.

For the present it will be assumed that the mirror reflection of the volume of Σ_c accessible by the backward angle experiment completely enclosed the volume of Σ_c accessible by the earlier, forward angle, experiment. This latter volume will be denoted V_f. Later, the validity of this assumption will be verified. A volume of phase-space mirror symmetric to V_f can also be defined and will be denoted V_b. A partial cross section was defined to be

$$\sigma_p = \int_V \frac{d^5\sigma}{d\theta^* d\phi^* d\psi d\chi dE_x} dV, \tag{10}$$

where V was the volume of interest—either V_f or V_b.

To compare the two experiments, the analysis of the present data was restricted to include only those events which fell inside V_b. Any which lay outside V_b were rejected. The remaining counts were summed to give an integrated yield into this volume. From this yield a cross section was calculated which could be directly compared to the cross section integrated over V_f as obtained from the earlier experiment. Although this phase space cut could in principle have been performed by calculating the position of each event in Σ_c and then comparing this to the volume of interest (V_b) this was not the best method in practice. To use such a method would have required a five-dimensional software gate. Instead, a simpler procedure was used. For each event, starting with its measured position in Σ_b, its location in Σ_c was calculated. A mirror reflection was performed on the event to give the equivalent event for the earlier experiment, and this new event was mapped to a position in Σ_f. It was much simpler to perform the phase-space cut in Σ_f as all that needed to be checked was that the two vectors $\mathbf{v_1}$ and $\mathbf{v_2}$ intersected the positions of the detectors in the earlier experiment. If, and only if, both vectors intersected the positions of the detectors then the point lay within V_f and hence the original event lay within V_b.

To summarize the method, due to the difficulty in quoting double differential cross sections, the cross section had to be

TABLE II. Excitation energy weighting functions used in the Monte Carlo simulation of phase-space coverage. All energy values are in MeV. It is energetically impossible to access excitation energies below 13.93 MeV or above 56.67 MeV.

Label	Function
E_a	1
E_b	$-(E_x-13.93)(E_x-56.67)$
E_c	$-(E_x-13.93)(E_x-56.67)e^{-(E_x-10/10)^2}$
E_d	$-(E_x-13.93)(E_x-56.67)e^{-(E_x-20/10)^2}$
E_e	$-(E_x-13.93)(E_x-56.67)e^{-(E_x-30/10)^2}$

integrated over mirror symmetric regions of the phase space. The events from the present experiment were filtered so that only those that were in the equivalent phase space matching the earlier experiment remained.

There was still the question of whether there was any phase space that could not be accessed in the present experiment that could be accessed in the earlier experiment. Figure 3 shows the results of calculations of phase-space coverage assuming the reaction occurred in a plane, that is with ϕ_1 and ϕ_2, and thus ϕ^* and χ, restricted to 0° and 180° only. Hence, the plots in this figure are of a three-dimensional slice through the five-dimensional center of mass phase space. Points with $\phi^*=180°$ have been shown with negative θ^*. Plot (a) in the figure shows a projection of the three-dimensional phase space along the θ^* axis onto the E_x-ψ plane. The two plots (b) and (c) show slices through the space for constant E_x. The two plots (d) and (e) show slices for constant ψ. It is clear from the figure that the overlap between the two experiments is good at low excitation energies but gets worse at higher excitation energies. The main reason for this is that the particle energies become too low to detect in the backward angle experiment as the excitation energy increases and as ψ moves away from 90°.

It was known from the forward angle experiment, that the measured yield of the reaction, at forward angles, was biased towards θ^* near zero. For both experimental setups, this tended to bias the measured yields towards low excitation energy and towards ψ near 90° as that was where the phase-space coverage of the experiments was closest to $\theta^*=0$.

Although the simple, in-plane, calculations could show that some of the phase space was missed, they were unable to quantify the volume. Instead, detailed Monte Carlo simulations were performed. These simulations were unrestricted in that they modeled out-of-plane as well as in-plane reactions. This was necessary as the finite vertical size of the detectors allowed events with ϕ_1 and ϕ_2 away from zero (and hence with ϕ^* and χ away from zero) to be detected. The method used was to pick points randomly from the full five-dimensional phase space, to determine if the point was accessible in the forward angle experiment and to determine if the mirror symmetric point was accessible in the backward angle experiment. This way the fraction of points accessible in the forward angle experiment but not accessible in the backward angle experiment could be estimated.

To account for the nonuniform distribution of the points due to the underlying reaction physics, weighting functions were used to bias the simulation to those regions of the phase space thought to be more likely to be accessed in the experiments. A selection of different weighting functions were used to determine the sensitivity of the calculations to the choice of function. The functions are shown in Tables II and III and Figs. 4 and 5. From Fig. 3 it can be seen that the calculations are only sensitive to the θ^* weighting between 0 and 20°. Comparison with efficiency corrected data from the forward angle experiment [12], suggested that the most realistic weightings were E_d and θ_c.

TABLE III. θ^* weighting functions used in the Monte Carlo simulation of phase-space coverage. All angles are in degrees.

Label	Function
θ_a	1
θ_b	$e^{(90-\theta^*/90)^2}$
θ_c	$e^{5(90-\theta^*/90)^2}$
θ_d	$e^{10(90-\theta^*/90)^2}$
θ_e	$e^{15(90-\theta^*/90)^2}$

The results of the Monte Carlo calculations are shown in Table IV. For the weighting combination E_d-θ_c, the calculations showed that approximately 22% of the phase space was missed in the backward angle experiment.

IV. RESULTS AND CONCLUSIONS

After performing the phase-space cuts as described earlier, an E_{tot} spectrum was generated for the events in the overlapping region of phase space, and is shown in Fig. 6(b). The ungated spectrum is shown again in Fig. 6(a) for comparison. While a Q_{ggg} peak corresponding to the $^{12}C+^{12}C+^{12}C$ final state is observed before gating, there is no clear evidence for such a peak after gating.

For the forward angle experiment, a value of (51

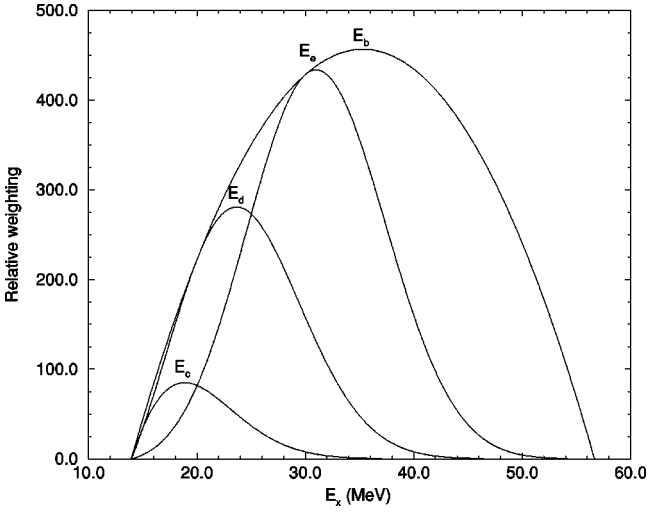

FIG. 4. Excitation energy weighting functions used in the Monte Carlo simulation of phase-space coverage. E_a has been omitted as it is equal to unity for all E_x.

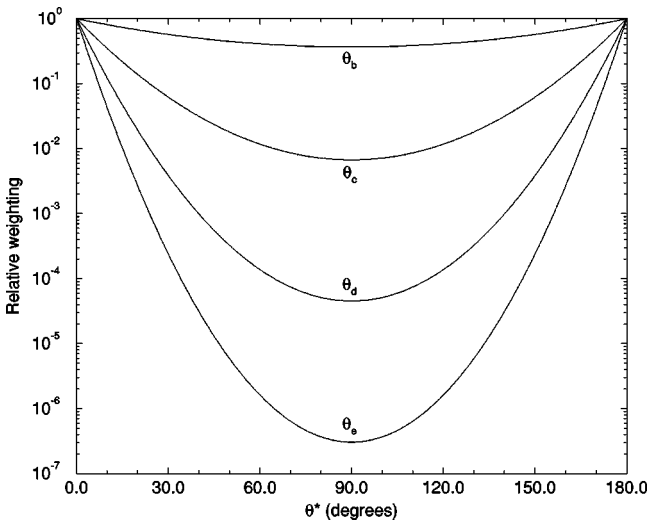

FIG. 5. θ^* weighting functions used in the Monte Carlo simulation of phase-space coverage. θ_a has been omitted as it is equal to unity for all θ^*.

$\pm 6)$ nb $[=(1.07\pm 0.12)\ \mathrm{mb\,sr^{-2}}\times\Delta\Omega_1\Delta\Omega_2]$ was measured for the cross section integrated over the experimental acceptance. This cross section had then to be corrected for the region of phase space inaccessible in the present experiment. This 22% correction reduced the coincidence cross section to (40 ± 5) nb. For a symmetric angular distribution, the same value should be obtained for the mirror symmetric region of phase space sampled in the backward angle data. In the present case, a cross section of 40 nb would correspond to approximately 800 counts expected in the Q_{ggg} peak after gating. A Gaussian line shape with this area, scaled down by a factor of 5 to fit on the figure, and with a width and centroid as given by the fit to the Q_{ggg} peak in the ungated E_{tot} spectrum, is indicated by the dashed curve in Fig. 6(b). As can be seen from the figure, the yield at backward angles is significantly lower than that expected for a symmetric angular distribution.

After gating, there are approximately ten counts in the region of the spectrum where the Q_{ggg} peak appears before gating. Allowing for $\sqrt{N}$ statistical fluctuations, then, at the 3 standard deviation level there could be at most 25 counts under the peak $(25-3\sqrt{25}=10)$. Subtracting the background

TABLE IV. Results of the Monte Carlo simulations. The figures are the percentage of the phase-space accessible in the forward angle experiment that could not be accessed in the backward angle experiment. The statistical counting errors on these figures are much less than 1%.

E_x	θ^* weighting				
weighting	θ_a	θ_b	θ_c	θ_d	θ_e
E_a	31%	30%	26%	21%	18%
E_b	40%	39%	33%	28%	24%
E_c	13%	13%	12%	11%	10%
E_d	26%	25%	22%	19%	17%
E_e	53%	51%	45%	38%	33%

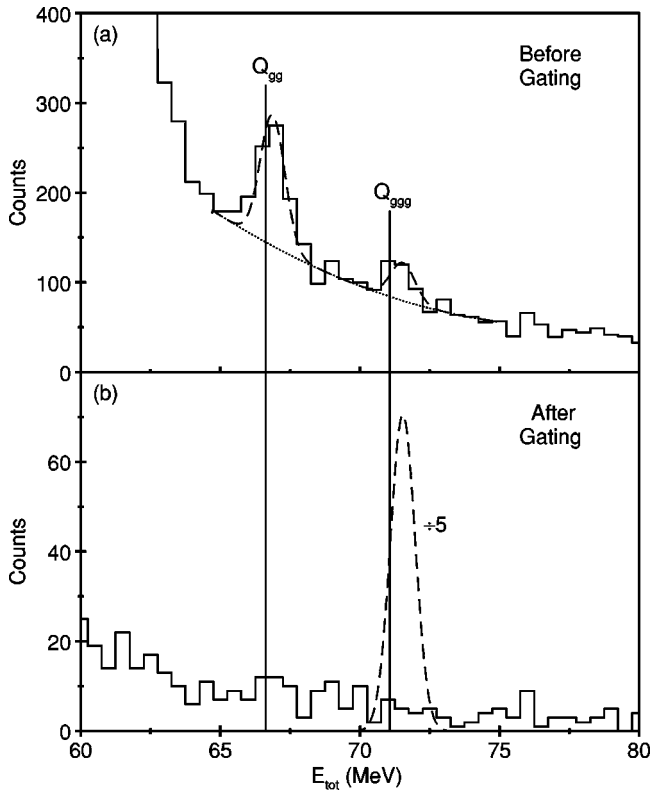

FIG. 6. E_{tot} spectra for the backward angle experiment showing (a) all data, and (b) only those data satisfying the forward angle criteria. Note that the energy dispersion has been changed from that in Fig. 1 to help to resolve the peaks. The Gaussian line shape in (b) indicates the Q_{ggg} peak expected for a symmetric angular distribution (see text). This peak has been scaled down by a factor of 5 to fit on the figure.

level of ten counts, this gives an upper limit of 15 counts in the peak. The upper limit used in calculations was 20 counts to allow for errors in the background estimate. This corresponds to an upper limit of 1.0 nb for the cross section at backward angles. It is emphasized that this is strictly an upper limit, partly due to statistical limitations, but more notably because no final-state interaction between the two ^{12}C nuclei has been identified. The data thus indicate that the angular distribution for the $^{12}\mathrm{C}(^{24}\mathrm{Mg},^{12}\mathrm{C}^{12}\mathrm{C})^{12}\mathrm{C}$ reaction is peaked at forward angles, with the yield at backward angles lower by at least a factor of 40.

The earlier work of Gyapong *et al.* [6] indicated that the energy variation of the breakup yield was consistent with either a resonant-type reaction proceeding through specific states in ^{36}Ar or direct inelastic excitation. A statistical compound reaction or massive ^{12}C transfer were found to be unlikely mechanisms on the basis of the observed energy dependence. The large difference between the measured yield at forward angles, 40 nb, and the upper limit of 1 nb observed in a mirror symmetric region of phase space at backward angles is inconsistent with the average behavior expected for a statistical compound nucleus reaction, which would imply an angular distribution symmetric about $\theta^*=90°$ [6]. A massive ^{12}C transfer mechanism, on the other hand, would naively be expected to preferentially produce

TABLE V. Optical model parameters describing the Woods-Saxon potential used in the coupled channels calculations, taken from Ref. [17].

Potential	V (MeV)	r_r (fm)	a_r (fm)	W (MeV)	r_i (fm)	a_i (fm)	r_C (fm)
CC1	169.2	5.02	0.6400	180.0	4.85	0.480	5.02

excited ^{24}Mg* nuclei moving backwards in the center of mass (relative to the original ^{24}Mg beam direction). Such an asymmetric angular distribution peaked at backward angles is also inconsistent with the present result, which therefore provides some support for the elimination of this mechanism by Gyapong *et al.*

Of the two possible reaction mechanisms found in Ref. [6] to be consistent with the observed energy dependence, only direct inelastic excitation is typically characterized by an asymmetric angular distribution peaked at forward angles. A compound nucleus reaction proceeding through overlapping resonances of different parity could, in principle, produce an asymmetric angular distribution because of interference between the different partial waves. Examples of this behavior for the $^{12}C + ^{24}Mg$ compound system are shown in Ref. [14]. However, the cross section quoted above for the forward angle data and the upper limit quoted for the backward angle cross section have implicitly been averaged over a wide range of scattering angles (typically $\theta^* = 0° \rightarrow 10°$) and, more importantly, over many final states in ^{24}Mg*. In such cases, interference effects between overlapping resonances are expected to average out to produce angular distributions, consistent with Hauser-Feshbach statistical model predictions, which are symmetric about 90° [15]. This is shown, for example, in the data of Ref. [16]. The asymmetry of the angular distribution reported in the present work thus suggests that direct inelastic excitation is the most likely reaction mechanism for the $^{12}C(^{24}Mg,^{12}C^{12}C)^{12}C$ reaction. If this is correct, then it would imply that the choice of ^{12}C as the target nucleus is not critical and it should be possible to excite the unusual cluster states by ^{24}Mg scattering from different target nuclei. Curtis *et al.* [17] have recently reported evidence for the $^{12}C + ^{12}C$ breakup of ^{24}Mg populated via the $^{16}O(^{24}Mg,^{12}C^{12}C)^{16}O$ reaction, which supports the interpretation that the cluster states are excited by direct inelastic scattering.

The spins of the $^{12}C + ^{12}C$ breakup states observed in the forward angle experiment range from 4^+ to 8^+ [10]. In terms of a direct inelastic scattering mechanism, these states would be expected to be populated by a multistep process, which may have an effect on the naive expectation of a forward peaked angular distribution. Therefore, coupled channels calculations have been performed to test whether the observed asymmetry is consistent with the inferred direct inelastic excitation mechanism.

The optical model parameters used in the calculations were taken from Ref. [17] and are reproduced in Table V. These parameters were fitted to data obtained for ^{12}C scattering from a ^{24}Mg target at a center-of-mass energy of 60 MeV, close to the center-of-mass energy of 56.7 MeV employed in the present work. The fit was performed simultaneously to differential cross sections measured for elastic scattering and inelastic scattering to the 2^+ (1.37 MeV) state in ^{24}Mg and the unresolved ^{12}C (2^+, 4.43 MeV) and ^{24}Mg (4^+, 4.1 MeV) states, allowing for two-way couplings between all states and including reorientation terms, Coulomb excitation and all angular momentum transfers up to $L = 4$. The deformation lengths thus obtained were $\beta R_{\text{g.s.}} = +1.491$ fm for the ^{24}Mg ground state band and $\beta R = -1.285$ fm for the ground state to 2^+(4.43 MeV) coupling in ^{12}C.

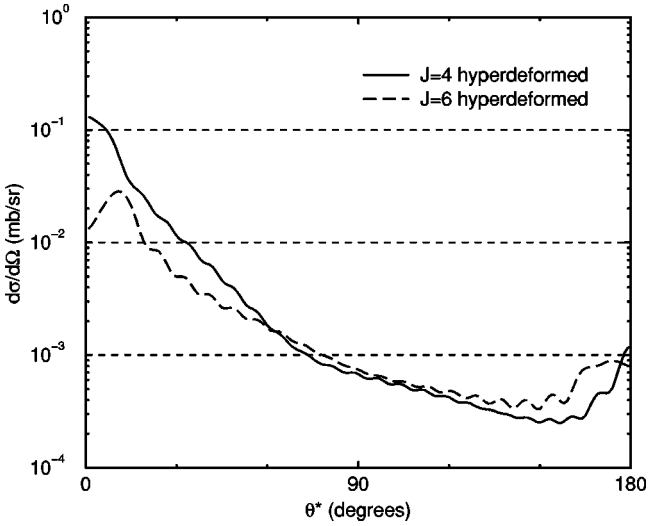

FIG. 7. Angular distributions for the 4^+ and 6^+ members of the hyperdeformed band, as obtained from the coupled channels calculations described in the text.

In the present calculations, as in Ref. [17], the breakup states have been modeled as a hyperdeformed rotational band with a rotational gradient $\hbar^2/2\mathcal{I}$ equal to the value observed experimentally [10]. A deformation length of $\beta R_{hd} = +2.495$ fm was chosen for this hyperdeformed band by scaling the value for the ground-state band according to the relative rotational gradients, assuming the moment of inertia $\mathcal{I}$ to be proportional to $(\beta R)^2$. The coupled channels calculations, performed using the code CHUCK99 [18,11], allowed for two-way couplings between the 2^+, 4^+, 6^+, and 8^+ members of the hyperdeformed band and included reorientation and Coulomb excitation. The couplings between the ground-state band and the hyperdeformed band were one way with a value $\beta R_{cross} = 0.1 \times \beta R_{hd} = 0.25$ fm chosen to ensure that the hyperdeformed band was not populated too strongly. Due to this arbitrary choice for the interband coupling, the calculated cross sections are subject to an unknown scaling factor, although this should not affect the conclusions drawn.

The angular distributions calculated for the 4^+ and 6^+ members of the hyperdeformed band, corresponding to the spins most strongly populated in the forward angle experiment [10], are shown in Fig. 7. The calculations predict for-

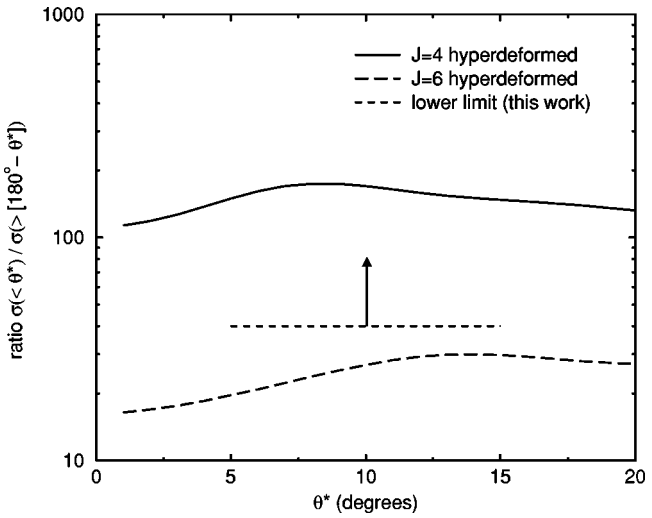

FIG. 8. Ratios of the cross sections at forward and backward angles, obtained by integrating the calculated angular distributions over equal angular ranges of $0° \rightarrow \theta^*$ and $180° - \theta^* \rightarrow 180°$, respectively, plotted as a function of θ^*. The experimental lower limit of 40:1 is also indicated.

ward peaked angular distributions asymmetric about $\theta^* = 90°$, as expected for a direct reaction mechanism. It is interesting to note, however, that the calculations predict a rise in cross section at backward angles (near 180°) which will have consequences for the relative yield at forward and backward angles. To investigate this further, the differential cross sections shown in Fig. 7 have been integrated over equal angular ranges starting at 0° and 180°, respectively, noting that $d\Omega = \sin\theta^* d\theta^* d\phi^*$. The forward angle experiment [12] was designed to be most sensitive to values of θ^* close to 0° (and breakup angles ψ close to $90°_{\text{c.m.}}$). While the precise acceptance is determined by simulations, a simple upper limit on the θ^* acceptance is a reasonable and transparent approximation. The ratios

$$\frac{\sigma(0° \rightarrow \theta^*)}{\sigma(180° - \theta^* \rightarrow 180°)}$$

of the calculated cross sections integrated over forward and backward angles are plotted in Fig. 8 as a function of the center-of-mass angle θ^* up to which the integration is performed. This ratio is not strongly dependent on the integration limit and hence the details of the angular acceptance have only a weak influence. Also indicated in Fig. 8 is the experimental lower limit of 40:1 obtained in the present work for the ratio of the breakup yield at forward and backward angles. The equivalent ratio predicted for the 4^+ member of the hyperdeformed band lies well above the experimental lower limit for all values of θ^* relevant to the present work (see Fig. 3), while that for the 6^+ state lies slightly below, peaking near $\theta^* = 14°$. However, the experimental ratio has been obtained by integrating over many states in ^{24}Mg, the most strongly populated of which have been assigned a spin of 4^+ [10], and hence the small discrepancy seen in Fig. 8 between the experimental lower limit and the ratio predicted for the 6^+ states is not significant. The observed ratio of the breakup yields at forward and backward angles thus appears to be consistent with the coupled channels calculations.

V. SUMMARY

The cross section of the ^{12}C(^{24}Mg,^{12}C^{12}C)^{12}C reaction at very backward angles has been measured by performing the experiment with reversed kinematics, that is, by performing a measurement of the ^{24}Mg(^{12}C,^{12}C^{12}C)^{12}C reaction at the same center-of-mass energy. The yield has been compared to a previous measurement of the reaction at forward angles.

The analysis was able to obtain a partial cross section for the reaction over a directly comparable region of phase space in the forward and backward angular regions. This was achieved by restricting the phase space spanned in the present measurement so as to include just the mirror symmetric region equivalent to the forward angle measurement. The region of phase space accessible in the earlier experiment, but not accessed in the present experiment, was estimated to account for only 22% of the cross section.

The total coincidence cross section was found to be (40 ± 5) nb at forward angles and <1 nb at backward angles indicating a strongly asymmetric angular distribution with the cross section being at least 40 times higher at forward angles than at backward angles. This factor would not be significantly influenced by an error in the estimate of unmeasured phase space. The upper limit on the backward angle cross section represents a limit in two separate senses. Whereas the present experiment clearly observed the ^{12}C + ^{12}C + ^{12}C final state as a Q_{ggg} peak, the subset of the data that was directly comparable with the forward angle experiment showed no statistically significant Q_{ggg} peak and a limit was estimated. In addition, while the forward angle experiment demonstrated a ^{12}C+ ^{12}C final-state interaction for events within the Q_{ggg} peak, implying the existence of states in ^{24}Mg, the low cross section at backward angles precluded a similar analysis in the present work.

A strongly asymmetric angular distribution is consistent with a direct reaction. Taken together with the earlier measurements of Gyapong *et al.*, this suggests that the reaction mechanism exciting cluster states is a direct inelastic excitation of the incident ^{24}Mg. The experimental lower limit of 40:1 for the relative cross section at forward and backward angles is consistent with the predictions of coupled channels calculations.

ACKNOWLEDGMENTS

The experimental work was carried out at the 14UD accelerator facility at the Australian National University (ANU) under a joint agreement between the ANU and the U.K. Engineering and Physical Sciences Research Council (EPSRC). The assistance of the personnel at the ANU is gratefully appreciated.

[1] B.R. Fulton, S.J. Bennett, C.A. Ogilvie, J.S. Lilley, D.W. Banes, W.D.M. Rae, S.C. Allcock, R.R. Betts, and A.E. Smith, Phys. Lett. B **181**, 233 (1986).
[2] J.S. Pople, N.M. Clarke, B.R. Fulton, M.J. Leddy, J.T. Murgatroyd, Y. Chan, R.G. Stokstad, W.D.M. Rae, W.N. Catford, S.P. Fox, G.J. Gyapong, D.L. Watson, and S.J. Bennett, Z. Phys. A **349**, 349 (1994).
[3] S. Marsh and W.D.M. Rae, Phys. Lett. B **180**, 185 (1986).
[4] M. Freer and A.C. Merchant, J. Phys. G **23**, 261 (1997).
[5] N. Curtis, N.M. Clarke, B.R. Fulton, S.J. Hall, M.J. Leddy, A.St.J. Murphy, J.S. Pople, R.P. Ward, W.N. Catford, G.J. Gyapong, S.M. Singer, S.P.G. Chappell, S.P. Fox, C.D. Jones, D.L. Watson, W.D.M. Rae, and P.M. Simmons, Phys. Rev. C **51**, 1554 (1995).
[6] G.J. Gyapong, D.L. Watson, W.N. Catford, N.M. Clarke, S.J. Bennett, M. Freer, B.R. Fulton, C.D. Jones, M. Leddy, J.T. Murgatroyd, W.D.M. Rae, and P. Simmons, Nucl. Phys. **A579**, 207 (1994).
[7] R. G. Stokstad, computer code STATIS, Technical Report No. 52, Yale University, 1974 (unpublished).
[8] W.D.M. Rae and A.C. Merchant, Phys. Lett. B **279**, 207 (1992).
[9] I.J. Thompson, Comput. Phys. Rep. **7**, 167 (1988).
[10] B.R. Fulton, S.J. Bennett, M. Freer, J.T. Murgatroyd, G.J. Gyapong, N.S. Jarvis, C.D. Jones, D.L. Watson, J.D. Brown, W.D.M. Rae, A.E. Smith, and J.S. Lilley, Phys. Lett. B **267**, 325 (1991).
[11] P. D. Kunz, computer code CHUCK, University of Colorado, 1974; J.R. Comfort, extended CHUCK3, University of Pittsburgh, 1979.
[12] M. Freer, Ph.D. thesis, University of Birmingham, 1991.
[13] N. Curtis, A.St.J. Murphy, M.J. Leddy, J.S. Pople, N.M. Clarke, M. Freer, B.R. Fulton, S.J. Hall, G. Tungate, R.P. Ward, S.M. Singer, W.N. Catford, G.J. Gyapong, R.A. Cunningham, J.S. Lilley, S.P.G. Chappell, S.P. Fox, C.D. Jones, D.L. Watson, P.M. Simmons, R.A. Hunt, A.C. Merchant, A.E. Smith, W.D.M. Rae, and J. Zhang, Nucl. Instrum. Methods Phys. Res. A **351**, 359 (1994).
[14] K. Daneshvar, W.K. Wells, D.P. Bybell, L. Mulligan, and D.P. Balamuth, Phys. Rev. C **25**, 1388 (1982).
[15] R. G. Stokstad, in *Treatise on Heavy Ion Science*, edited by D. A. Bromley (Plenum, New York, 1985), Vol. 3, p. 83.
[16] L.R. Greenwood, K. Katori, R.E. Malmin, T.H. Braid, J.C. Stoltzfus, and R.H. Siemssen, Phys. Rev. C **6**, 2112 (1972).
[17] N. Curtis, M. Shawcross, W.N. Catford, B.R. Fulton, N.M. Clarke, S.J. Hall, J.T. Murgatroyd, S.P.G. Chappell, R.L. Cowin, G. Dillon, and D.L. Watson, Phys. Rev. C **61**, 064606 (2000).
[18] N.M. Clarke, CHUCK99, University of Birmingham, 1999.